PHYSICAL REVIEW B VOLUME 35, NUMBER 9 15 MARCH 1987-II

Radiation effects and anelastic loss in germanium-doped quartz

Ferdinand K. Euler and Alfred Kahan
Solid State Sciences Division, Rome Air Development Center, Department of the Air Force, Hanscom Air Force Base, Massachusetts 01731

(Received 8 September 1986; revised manuscript received 24 November 1986)

5-MHz resonators were fabricated from germanium-doped cultured quartz and were ^{60}Co irradiated at room temperature. The quartz has a relatively low aluminum-impurity concentration, 0.5 ppm, and the aluminum is lithium compensated. Oscillator frequency offsets $\Delta f/f$ and resonator anelastic loss spectrum Q^{-1} were measured and show an increase and subsequent decrease as a function of dose, known as radiation bleaching. At low irradiation levels, $\Delta f/f$ decreases with increasing dose, reaches at 50 krad a minimum of -4×10^{-7}, reverses and increases with additional dose, and at 1 Mrad it recovers to -1.2×10^{-7}. (1 rad$\equiv$100 ergs/g.) These values are surprisingly large in comparison with other lithium-compensated high-quality quartz. Resonator irradiation induces a Q^{-1} peak centered at 246 K, which also bleaches with radiation. At 246 K the Q value is 2.25×10^{6}, decreases with irradiation, reaches at 50 krad a minimum of 0.65×10^{6}, and recovers at 350 krad to 1.5×10^{6}. Electron paramagnetic resonance (EPR) measurements show Al hole, and germanium C and A centers, Ge(C)-Li and Ge(A)-Li, neutral defects of a trapped electron localized on a substitutional Ge site and stabilized by an adjacent Li^{+} ion. All three EPR spectra also radiation bleach at doses above 50 krad. This strongly suggests that the Ge(C)-Li defect is associated with the 246-K loss peak. The activation energy of the Q^{-1} peak is $E=0.22$ eV, the corresponding relaxation time $\tau_0=8\times10^{-13}$ sec, and the peak anneals at 555 K.

INTRODUCTION

The frequency of a quartz resonator is determined by crystal thickness, shape, mounting, and a combination of material constants including the elastic, dielectric, piezoelectric, and thermal-expansion coefficients. Resonators fabricated from quartz are used in high-precision oscillators and may have to operate in a radiation-permeated environment. Irradiating the resonator causes transient and steady-state frequency offsets. In resonators fabricated from high-quality quartz these effects are attributed to redistribution of impurities and other point defects which alters material constants and causes a resonator frequency shift.[1–5]

The major impurity associated with radiation-induced frequency offset is an aluminum ion Al^{3+}, substitutional at a silicon Si^{4+} site. Before irradiation, Al^{3+} is charge compensated by a monovalent interstitial alkali-metal ion M^{+}, denoting lithium, sodium, or potassium, and after irradiation by a proton, or by the removal of an electron from a nonbonding orbital of a neighboring oxygen anion. Alkali-metal compensators form Al-M^{+} pairs, H^{+} forms an OH^{-} near Al^{3+}, and the missing electron forms an Al-hole (h) center. We designate these defects as Al-M (Al-Li, Al-Na, Al-K), Al-OH, and Al-h, respectively. The point-defect structure of quartz and its modification by ionizing radiation are reviewed by Griscom,[6] Weil,[7] and Halliburton and Martin.[8]

Another set of point defects is formed by Ge^{4+} isomorphously replacing Si^{4+} in the SiO_4 tetrahedron. Irradiating a sample produces electrons and holes which move through the crystal until they recombine or are trapped by impurity centers. The free electron is trapped by the germanium, and the free hole forms Al-h. At room temperature, the M^{+} ion diffuses from Al-M and stabilizes the Ge-defect site forming $[\mathrm{Ge}(A)e^{-}/M^{+}]^{0}$ and $[\mathrm{Ge}(C)e^{-}/M^{+}]^{0}$, with $M^{+}=$Li or Na. These centers are designated here as Ge(A)-Li and Ge(C)-Li, and Ge(A)-Na and Ge(C)-Na.[9–12]

Radiation effects associated with sodium compensated Al^{3+} are more severe than those associated with lithium or hydrogen.[1,13] Sodium in quartz is virtually eliminated by adding a lithium compound during crystal growth. In a grown crystal both Li^{+} and Na^{+} ions are removed by electrodiffusion (sweeping). The M^{+} compensators are physically "swept" from the crystal and exchanged with a proton. Both techniques were developed by King and his co-workers and have been adopted in industrial growth and processing of high-quality cultured quartz.[14–17]

A combination of material characterization and resonator evaluation techniques, including dielectric or anelastic loss spectra, infrared spectroscopy, and electron paramagnetic resonance (EPR) are known for identifying specific precursors and trapping centers responsible for radiation-induced frequency offsets. The general theory and results of low- and high-temperature anelasticity, or internal friction Q^{-1}, are reviewed by Fraser.[18,19] Other anelastic loss studies on unswept, swept, and irradiated quartz are reported in Refs. 1, 13, and 20–22. This technique has been successfully applied in the study of Al-Na, characterized by two low-temperature Q^{-1} relaxation peaks. Hydrogen-related centers, grown-in OH and Al-OH, are studied by low-temperature near-infrared spectroscopy.[23–25] EPR has been extensively applied in the study of Al-h and other Al and Ge defects[9–11,26,27] and is reviewed by Weil.[7]

Work of the U. S. Government
Not subject to U. S. copyright

Industrially grown quartz has aluminum concentrations of 1–15 ppm.[28] Doherty *et al.*,[29] Armington and Balascio,[30] and Armington and Larkin[31] reported on growth programs for high-quality low-aluminum-content quartz. They show that by a combination of techniques the aluminum concentration can be reduced to 10–100 ppb. In this investigation we are reporting on the radiation sensitivity of frequency and anelastic loss of resonators fabricated from one batch of high-purity quartz grown by Armington and his co-workers. This material has an aluminum impurity concentration of 0.5 ppm and low dislocation density. However, owing to contamination from a previous growth run, it became, unintentionally, Ge doped. Previous studies of radiation-induced steady-state frequency offset ignore the influence of Ge defects. This is either due to the fact that in cultured quartz aluminum is, but germanium is not a contaminant, or that germanium effects are unrecognized or overshadowed by aluminum contributions. We have then the opportunity to investigate the radiation sensitivity of low-aluminum Ge-doped quartz and to possibly separate Al- and Ge-impurity effects.

EXPERIMENTAL PROCEDURES

Quartz bars evaluated in this investigation were grown at the Rome Air Development Center (RADC) hydrothermal facility, run QA-38. X-ray transmission topography of a Y plate indicates that the Z-growth region is almost dislocation free.[32] Atomic absorption analysis shows the aluminum impurity to be 0.5 ppm. EPR analysis shows that aluminum concentrations are symmetric on the two sides of the seed, have average values of 0.55 ppm, and decrease by 30% from the seed towards the outer surface.[31,33] This magnitude of aluminum impurity variation is normal in high-quality quartz.[25] Low-temperature infrared spectroscopy, at 80 K, confirms the Al-impurity concentration and distribution.[34] Infrared results also indicate that the grown-in OH concentration is sufficient to proton compensate all dissociating Al-M defects.[35]

Chemical analysis showed a relatively large concentration of germanium, ≈ 30 ppm. EPR data also indicates the presence of radiation-induced Ge defects, Ge(A)-Li and Ge(C)-Li. The EPR strength of these centers has not been calibrated in terms of germanium concentration. Infrared spectra do not show any novel peaks, or unusual peak strengths, which could be attributed to Ge defects. An examination of the autoclave record showed that Ge-doped quartz was grown two runs prior to QA-38. Despite thorough cleaning after each run by standard procedures, the autoclave was still contaminated and the quartz become unintentionally Ge doped.

One crystal was lumbered into two pure Z-growth bars. The Z faces of one bar were platinum plated and the bar swept in air ambient. Resonator units fabricated from the two bars at Frequency Electronics, Inc. (FEI) were 5 MHz, fifth overtone, AT cut, biconvex, gold electroded, and thermal compression bonded. We are reporting measurements on three resonators from QA-38 which we designate as resonators 1, 2, and 3, and on two resonators from the QA-38 swept bar which we designate with the suffix s. We also measured resonators fabricated from SARP Premium-Q quartz, run D14-45, utilized in previous ^{60}Co and 10-MeV pulsed electron linear accelerator (linac) irradiation experiments.[20,36] Compared to other Premium-Q material, D14-45 has a low aluminum impurity concentration, 1 ppm.[25]

Three measurement sets, covering temperature ranges 12–295, 200–360, and 295–400 K, were used to measure resonant frequency f and resistance R as a function of temperature T. The first set utilizes a closed-cycle helium-gas refrigerator, the second a liquid-nitrogen (LN) cooled temperature chamber, and the third a small electric furnace. The temperature rise in the helium-gas refrigerator was uncontrolled with rates decreasing from 0.9 to 0.05 K/min, in the LN chamber it was cam controlled with rates between 0.5 and 0.6 K/min, and in the electrically programmed oven it was 0.3 K/min.

Resonator terminals were connected with 50-Ω coaxial cables through a π network to a Hewlett-Packard HP35570 network analyzer. Cable length was minimized as much as possible. An HP3330 programmable synthesizer served as the frequency source. The controlling software tracked the resonance and measured the output signal magnitude as a function of frequency with preselected timing. Resonant resistance was derived from the maximum magnitude, and resonant frequency was defined by the zero slope at maximum magnitude. Resonator irradiations were performed at the RADC 43 000-Ci ^{60}Co facility. Resonators were irradiated incrementally in the passive mode and $R(T)$ measured after each radiation exposure. Dose and dose rate accuracies range from $\pm 0.5\%$ to ± 2–3%.

Frequency offset as a function of radiation dose was also measured in an active oscillation mode. The oscillators were operated continuously at resonator turnover temperatures for 10 d. Aging rates of oscillator frequencies, after this adaptation period, ranged from -1×10^{-10} to $+4\times10^{-10}$ per day. In the oscillator testbeds utilized for these irradiations, the resonator is located at one end of the unit. This allows resonator exposure and, at the same time, circuit element shielding. For calibration, the dose rate was measured at the resonator position inside the empty shielding structure. The dosimetry error of this procedure is estimated to be twice that for the passive resonators.

Irradiation levels were selected to evaluate effects of low, intermediate, and high dose exposures. The initial irradiation increments were 1, 2, 7, and 10 krad, at a dose rate of 0.6 krad/min. (1 rad $\equiv$ 100 ergs/g.) After each exposure the oscillator frequency was allowed to recover for 30 min to 1 h. At the completion of this sequence, the frequencies recovered for 2 d. The oscillators were then exposed again to the same sequence. After an additional 15-d recovery the oscillators were irradiated with 10-, 40-, 110-, 250-, and 550-krad increments at dose rates ranging from 7.9 to 9.3 krad/min. Recovery periods between these increments ranged from 1 to 16 h.

The oscillator frequency was mixed with the output of a Fluke 6160B synthesizer set to 4.999 MHz, and the resulting beat frequency measured by a Hewlett-Packard

HP5345 electronic counter. Synthesizer and counter frequencies were referenced to a Frequency Electronics FE150A disciplined frequency standard. The frequency measurements during exposures were averaged over time intervals of 20 or 30 sec, and over 200 sec during the long-term recovery periods. The observed short-term fluctuations were in the order of $\pm 3\times 10^{-11}$.

RESULTS

Figure 1 shows normalized steady-state oscillator frequency offset $\Delta f/f$ as a function of accumulated ^{60}Co dose, for resonators fabricated from unswept and swept crystals. The solid and open circles denote measurements made after the short and long recovery periods, respectively. It was found that from about 1 d after irradiation, the frequency changes at rates commensurate with preirradiation aging. The $\Delta f/f$ values of QA-38 resonator 1 are negative, decrease between 20 and 80 krad to a minimum of -4×10^{-7}, and reverse with additional dose, reaching -1.3×10^{-7} at 1 Mrad. After an additional 15 d of recovery the offset is -1.1×10^{-7}. For the D14-45 quartz resonator the maximum frequency offset also occurs between 20 and 60 krad, but is smaller by a factor of 6, in general agreement with previously tested resonators from this material.[36]

Figure 1 also shows measurements on resonators fabricated from swept quartz QA-38s and D14-45s1 and D14-45s2. Suffixes s1 and s2 denote two different resonators. For QA-38s the sweeping process reduces the overall radiation sensitivity by about a factor of 20, and flattens the dose dependence. After 1 Mrad and 15-d recovery $\Delta f/f$ changed from -0.9×10^{-8} to $+1.2\times 10^{-8}$, and the aging rate did not return to its preirradiation value. Data from a second QA-38s resonator, not shown in Fig. 1, is very similar. Frequency offsets for resonator D14-45s are also in the 10^{-9} range. The difference between D14-45s1 and D14-45s2, negative versus positive offset, may not be intrinsic to the material but may reflect fabrication differences and sweeping procedures. In previous passive-mode resonator tests, D14-45s exposed to 1 Mrad ^{60}Co showed $\Delta f/f$ between -0.5×10^{-8} and -2×10^{-8}, and in active-mode oscillators, after 1 Mrad of 10-MeV electrons, $\Delta f/f$ was $+1.2\times 10^{-8}$, in close agreement with current findings.[36]

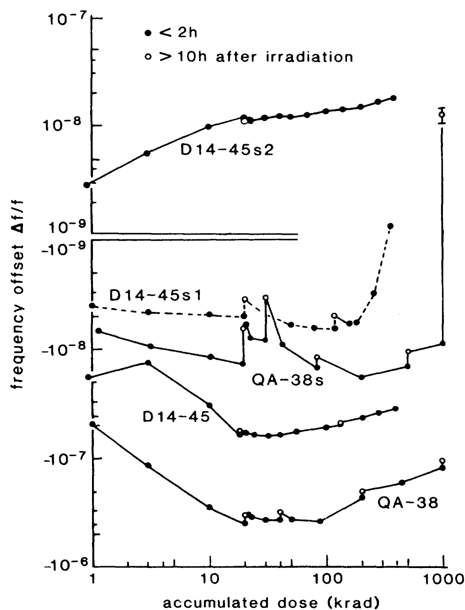

FIG. 1. Radiation-induced steady-state frequency offset $\Delta f/f$ as a function of accumulated dose of resonators fabricated from Ge-doped QA-38 and Premium-Q D14-45 quartz. Suffix s denotes crystals swept in air ambient. QA-38 data is of resonator 1.

Figure 2 shows passive resonator irradiation data of QA-38 resonator 2. The relative resonant frequency $df/f_n=(f-f_n)/f_n$, nominal frequency $f_n=5$ MHz, is shown as a function of temperature before and after a 26-krad irradiation. The curves exhibit the cubic characteristic of AT-cut crystals, and the two insets show, on an enlarged scale, df/f_n at the lower and upper turnover. For the irradiated sample, the frequency starts deviating around 230 K, attains the maximum offset -9×10^{-7} at 250—260 K, and retains this difference at higher temperatures, including the upper turnover. Figure 1 showed that after a comparable radiation dose in the active oscillator mode, the frequency offset is -4×10^{-7}. This smaller active-mode offset is consistent with our previous experience and attributed to the effect of oscillator circuit elements on crystal resonant frequency.

Figure 3 shows resonance resistance between 200 and 380 K as a function of accumulated dose for QA-38 resonator 2. The right-hand scale shows corresponding Q^{-1} values, calculated from

$$Q^{-1}=R/(2\pi f_n L)=(R/80\pi)10^{-6} \quad (1)$$

with $f_n=5$ MHz, and $L=8$ H, the average value found from measurements above room temperature. Unirradiated resonator resistance is 110 Ω, with weak resistance peaks between 270 and 360 K, due to coupled spurious mode resonances. Irradiation introduces a major loss peak at 246 K. This peak grows initially with increasing

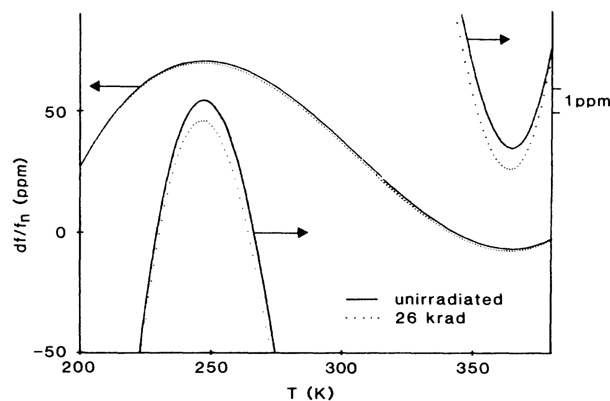

FIG. 2. Relative resonant frequency df/f_n, referenced to $f_n=5$ MHz, as a function of temperature T of QA-38 resonator 2. The enlarged-scale insets show the radiation-induced differences near the lower and upper turnover temperatures.

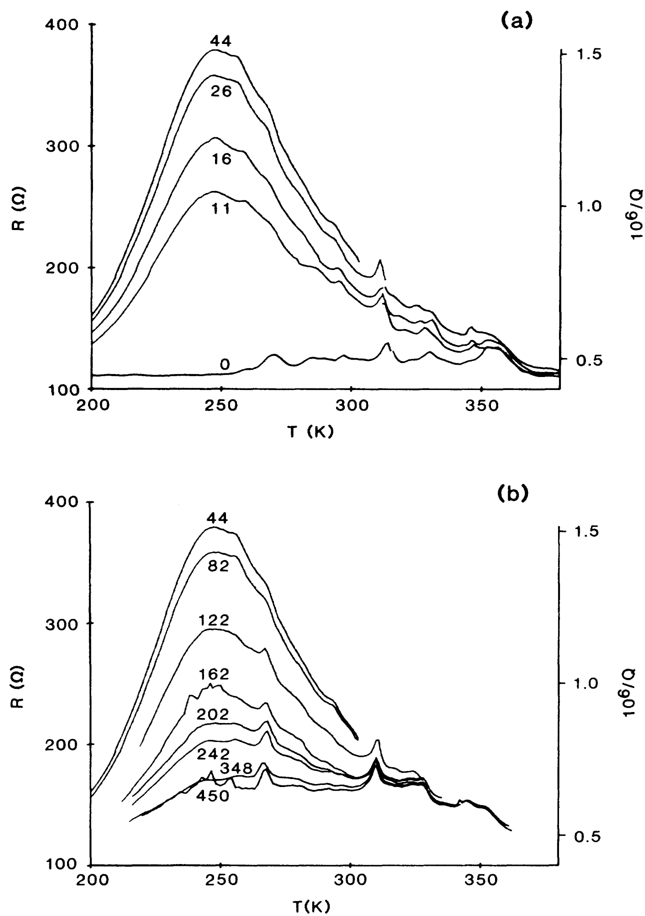

FIG. 3. Resistance R and anelastic loss Q^{-1} as a function of temperature T of QA-38 resonator 2. The labels for each curve indicate the accumulated dose in krad.

dose, reaches a maximum of 380 Ω at 44 krad, and decreases at higher doses to 160 Ω at 450 krad. At maximum loss, the equivalent Q value is reduced from 2.25×10^6 to 0.66×10^6.

The high-dose radiation data also shows the growth of a broad secondary band centered around 290—320 K, which overlaps the 246-K peak. This broad band may be identical with the 305-K Li defect observed by Martin.[37] We also measured the Q^{-1} spectra of irradiated resonators fabricated from swept QA-38 quartz. These do not show the 246-K loss peak and the broad 290—320 K centered band.

We studied the 246-K loss peak annealing characteristics. Owing to fabrication processes, resonator temperatures are constrained to below 570 K. Figure 4 shows resistance as a function of temperature for QA-38 resonator 3, unirradiated, after 21 krad, and after 555-K heat treatment for 1 h. The 246-K peak has annealed, but the higher temperature band centered at 290—320 K is still present. The data also shows the shifting of the spurious and anharmonic modes with radiation or anneal. Complete annealing of the 246-K loss peak was also observed after 555-K heat treatment for QA-38 resonator 1, irradiated with 1 Mrad. QA-38 resonator 2 was annealed at

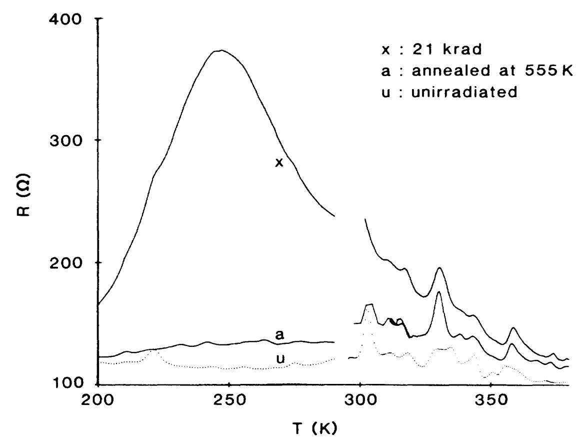

FIG. 4. Resistance R as a function of temperature T of QA-38 resonator 3. The data gap near room temperature is due to using two nonoverlapping measurement sets.

555 K and reirradiated to 10.7 krad. The 246-K loss peak annealed and was reintroduced with 70% of its former value for the same dose. The resonator was then subjected to 30-min isochronal anneals. Figure 5 shows the unannealed fraction of peak resistance as a function of anneal temperature. There is a small annealing stage below 450 K, and a gradual annealing between 470 and 555 K.

DISCUSSION

Frequency offsets

The frequency offsets of resonators fabricated from crystal QA-38 are surprisingly large in comparison to other lithium-compensated high-quality quartz. Chemical analysis, infrared spectroscopy, and EPR measurements all show that QA-38 is indeed a material of low aluminum concentration, 0.55 ppm, compared to the best Premium-Q D14-45, 1 ppm. However, the maximum frequency offset of QA-38 is six times larger than for D14-45. Another anomaly with QA-38 is the frequency-offset reversal with increasing dose, known as radiation bleaching. We are unaware of any other oscillator radiation experi-

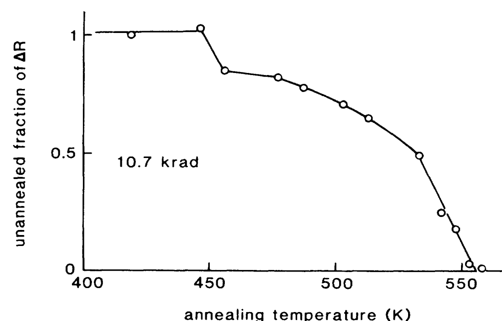

FIG. 5. Unannealed fraction of the radiation-induced peak resistance change at 246 K as a function of annealing temperatures after 10.7 krad irradiation of QA-38 resonator 2. Isochronal anneal times were 30 min.

ment which shows such a large magnitude of radiation bleaching.

King showed that, in a first approximation, there exists a direct correlation between radiation-induced frequency offset and Q^{-1} changes below operating temperature.[13] The frequency offset caused by the complete relaxation of a single loss mechanism is equal to the change in the maximum value of the loss, $\Delta(df/f)=\Delta Q_m^{-1}$. By sweeping sodium into a sample, Fraser showed that the 50-K loss peak, at 5 MHz, is associated with Al-Na.[18] Introducing a 50-K peak with $\Delta Q_m^{-1}=7\times10^{-4}$ also changed df/f at the upper turnover, 90 °C, by 7×10^{-4}, confirming King's relationship for Na-swept quartz. King's relationship is also corroborated for the 246-K peak. After 26 krad irradiation, ΔQ_m^{-1} is 9.8×10^{-7} and $\Delta(df/f)$ at the upper turnover is 9×10^{-7}. The agreement between ΔQ_m^{-1} and $\Delta(df/f)$, the fact that the frequency offset is introduced between 230 and 250 K, and the parallel radiation bleaching observed in oscillator frequency and Q^{-1} spectra, all indicate that the frequency offset and the 246-K peak are caused by the same defect center.

Anelastic loss peaks

Martin showed radiation-induced broad weak Q^{-1} bands at 305 or 340 K for quartz into which lithium or sodium was swept.[37] These bands grow as a function of dose, and either saturate or decrease in strength after reaching a maximum between 40 and 80 krad. It is possible that the 290—320 K centered band observed in this investigation is related to the band observed by Martin. Based on the fact that the 246-K peak was not induced in Martin's experiments, and that it anneals differently from the 290—320-K band, we may conclude that these signatures reflect different defects.

A radiation-induced Q^{-1} peak in the vicinity of 250 K, or its equivalent dielectric loss peak, is not discussed in the literature. Capone *et al.*[1] showed the existence of a peak in this temperature region after 1 Mrad linac irradiation in high-quality selected natural quartz, and in cultured quartz grown with lithium nitride and lithium carbonate, but they did not comment on its origin. Since Q^{-1} was measured only before and after 1 Mrad, the dose dependence of this peak was not observed.

One possible reason for the large frequency shifts in QA-38 is that the lithium additive might have been omitted during crystal growth introducing sodium into the crystal. We measured the low-temperature Q^{-1} spectra of QA-38, but did not find any Al-Na, or any other impurity-related, peaks. We cannot associate the 246 K peak with any identified anelastic or dielectric loss defect. We consider Al-K as a possibility. At 5 MHz Al-K has a loss peak at 208 K and an activation energy of $E=0.25$ eV.[18] However, the temperature discrepancy is too large for experimental error. Stevels and Volger[38] and Stevels[39] have attributed several dielectric loss peaks found at 32 kHz to specific impurities. We calculated the corresponding 5-MHz temperature positions of these peaks, and they do not fall in the 246-K range. Also, to the best of our knowledge there are no reported Q^{-1}, or dielectric loss, peaks associated with Ge-defect sites.

The different annealing characteristics of the 246-K peak and the partially overlapping higher-temperature band centered at 290-320 K allow us to separate contributions of the two mechanisms and calculate the activation energy of the 246-K loss peak. The internal friction Q^{-1} is given by

$$Q^{-1}=D\frac{\omega\tau}{1+(\omega\tau)^2}\,, \tag{2}$$

where D is the relaxation strength and $\omega=2\pi f$, where f is the resonant frequency. The relaxation time of the loss process is defined by $\tau=\tau_0\exp(E/kT)$, where τ_0 and kT have their usual meaning, and E is the activation energy.[13,19] It can be shown that $D=2Q_m^{-1}$, where Q_m^{-1} is the maximum value. The normalized Q^{-1} becomes

$$Q^{-1}/Q_m^{-1}=1/\cosh(u)\,, \tag{3}$$

where

$$u=E/(1/kT-1/kT_m) \tag{4}$$

and T_m is the temperature at Q_m^{-1}.

Figure 6 shows the theoretical fit to ΔR, the resistance differences between the 21-krad-irradiated and 555-K-annealed curves depicted in Fig. 4. A least-squares fit of this curve yields $T_m=246.3$ K and $E=0.220$ eV. The calculated τ_0 is 7.7×10^{-13} sec. These values are reasonable when compared with activation energies of other impurity-related defect centers.[38] Figure 6 also shows the residuals between the fitted and measured data. Most of the differences can be attributed to contributions of spurious modes, which were present before and after irradiation but annealed or shifted after the 555-K heat treatment. The excellent fit suggests strongly that the 246-K loss is due to a single defect mechanism. The 246-K peak is absent in resonators made from swept QA-38 quartz, and thus the defect appears to be associated with an interstitial alkali metal, lithium, compensating a substitutional ion.

Germanium-lithium defects

EPR studies of room-temperature irradiated Ge-doped quartz identify two sets of signals associated with

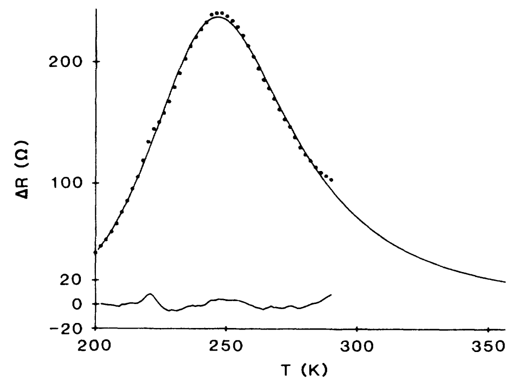

FIG. 6. Resistance change ΔR as a function of T of QA-38 resonator 3. Dots denote the measured and the solid line the fitted values. The bottom curve shows the residuals between measured and fitted values.

Ge(C)-Li and Ge(A)-Li, and two corresponding sets for the sodium analogs of these defects.[9–11,40,41] All investigations agree that for Li^+ compensation the C center, and for Na^+ compensation the A center, is the dominant defect. Anderson and Weil also show the growth and subsequent decay of these signals as a function of x-ray irradiation time.[10] Annealing of the EPR spectra associated with Ge(C)-Li have been reported and show annealing between 450 and 600 K.[42] Annealing stages are not well defined, and there are very large sample-to-sample variations. However, it was concluded that annealing is dominated by electron-hole recombination, electrons released from Ge(C)-Li recombine with holes at Al-h. Halliburton *et al.* showed that in Ge-free samples Al-h anneals between 500 and 600 K.[26] The 246-K loss peak annealing results are in general agreement with these findings.

In order to establish a relationship between the 246-K loss peak and a Ge defect, we checked the radiation bleaching characteristics of EPR signals.[33] Doses were chosen to coincide with radiation exposures of the passive resonator. Table I lists the doses, Al content and Al-h both in ppm and normalized to sample Al concentration. An inspection of this column shows that less than 60% of the Al sites form Al-h. The last two columns show the strength of Ge(C)-Li and Ge(A)-Li. The EPR signal of the A center was considerably weaker than that of the C center. The scales in Table I for these two centers have been normalized to yield a common maximum strength of 0.31 to compare with the maximum Al-h concentration of 0.31 ppm.

Figure 7 shows a plot of the EPR signal strength of the three centers as a function of dose. It also shows the radiation-induced loss change ΔQ_m^{-1} at 246 K, data from Fig. 3. All four data sets show similar dose dependence, a rise to maximum values occurring near 50 krad and similar degrees of radiation bleaching at higher doses. These data then indicate a close correlation between the defect giving rise to the 246-K Q^{-1} loss and the EPR-determined centers. We are unaware of any other EPR, or optical data, on Ge-doped or Ge-free samples which show radiation bleaching of Al-h. In this plot ΔQ_m^{-1} includes contributions from the 290–320 K centered band. In order to determine the generation of the pure 246-K peak, we would have to subtract at each dose not the unirradiated but the 555-K annealed values. Such measurements were performed only after the 21 krad on resonator 3 and after 450 krad on resonator 2, yielding the corrections $(0.04-0.08)\times 10^{-6}$ and 0.03×10^{-6}, respectively.

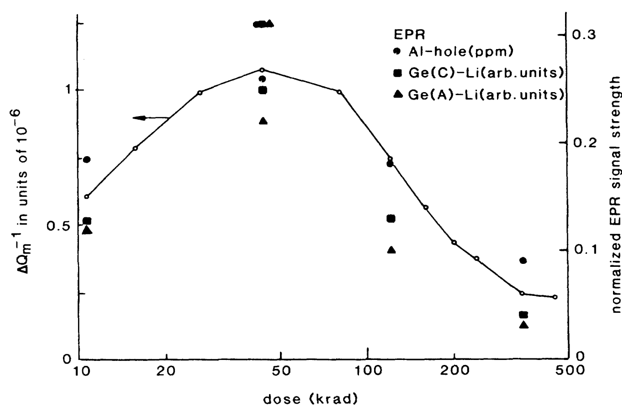

FIG. 7. Radiation-induced loss change ΔQ_m^{-1} at 246 K of QA-38 resonator 2, and normalized EPR signal strength of Al-hole, Ge(C)-Li, and Ge(A)-Li as a function of accumulate dose.

Figure 8 shows the strength of the two Ge-Li centers as a function of Al-h concentration. For these defect concentrations there is a linear relationship between Al-h and both Ge(C)-Li and Ge(A)-Li. This is one more manifestation of the common mechanism involving the three centers. Based on all these considerations we associate the 246-K peak with Ge(C)-Li, the dominant center in Li^+-ion-doped samples. Toulouse and Nowick[43] showed that in order to observe anelastic or dielectric relaxation the interstitial alkali-metal ion has to reside off the twofold symmetry axis. For the Al-M defect, Na^+ is off and Li^+ is on the twofold axis. The identification of the 246-K peak with Ge(C)-Li then requires that Li^+ is situated off the twofold axis when associated with Ge. This would then explain the large radiation sensitivity observed for Ge-doped samples, similar to Al-Na.

Radiation bleaching

Radiation bleaching, the generation and subsequent decay of a radiation-induced defect center with increasing dose, has been analyzed by Paige[44] for a neutron-induced hole center. Paige invokes the interaction of three defect centers, one electron and two hole traps. In a quartz sample, which has aluminum impurities, but is germanium free, Al^{3+} is compensated with M^+ ions. Irradiation forms both Al-h and Al-OH and removes M^+-ion compensators which diffuse to other sites. Charge neutrality

TABLE I. Defect-center concentrations of EPR samples.

Sample	Dose (krad)	Al content (ppm)	Al-hole (ppm)	Al-hole fraction (%)	Ge(C)-Li	Ge(A)-Li
C	11	0.63	0.185	29	0.13[a]	0.12[a]
A	44	0.46	0.26	57	0.25	0.22
F	44	0.67	0.31	46	0.31	0.31
D	122	0.45	0.18	40	0.13	0.10
E	350	0.55	0.09	16	0.04	0.03

[a]Arbitrary units normalized to yield identical maxima for the three centers.

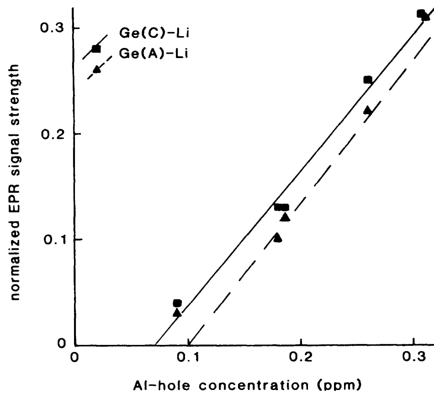

FIG. 8. Normalized EPR signal strength of Ge(*C*)-Li and Ge(*A*)-Li as a function of Al-hole concentration.

implies the existence of an electron trap. This trap has not been identified. It is likely that, similar to Ge(*C*)-Li, the electron trap is stabilized by the diffusing alkali metal. For the radiation bleaching of an electron center, we assume, in reverse analogy to Paige, the existence of one hole and two electron traps. We designate the hole trap as the H defect, and the two electron traps as the C defect and the D defect. We associate the H defect with Al-h, the C defect with Ge(*C*)-Li, and the D defect with the unidentified electron trap which apparently exists independent of germanium impurity.

Irradiating a sample generates free electron-hole pairs which are subject to recombination and trapping processes. The rate equations governing the free and trapped carrier concentrations as a function of irradiation time t are

$$dn/dt = X - C_1(N_c - n_C)n - D_1(N_D - n_D)n - H_2 p_H n - kpn \ , \tag{5a}$$

$$dp/dt = X - H_1(P_H - p_H)p - C_2 n_C p - D_2 n_D p - knp \ , \tag{5b}$$

$$dp_H/dt = H_1(P_H - p_H)p - H_2 n p_H \ , \tag{5c}$$

$$dn_C/dt = C_1(N_C - n_C)n - C_2 p n_C \ , \tag{5d}$$

$$dn_D/dt = D_1(N_D - n_D)n - D_2 p n_D \ . \tag{5e}$$

Charge neutrality requires

$$n + n_C + n_D = p + p_H \ , \tag{5f}$$

$$N_C + N_D = P_H \ . \tag{5g}$$

In these equations, we define n and p as densities of free electrons and holes, and densities n_C, n_D, and p_H of electrons trapped at C and D and of holes trapped at the H sites. The rate constants are defined as follows: X, electron-hole pair generation; k, direct electron-hole recombination; H_1, hole trapping at H sites; H_2, free-electron recombination with holes trapped at H sites; C_1, electron trapping at C sites; C_2, free-hole recombination with electrons trapped at C sites; D_1, electron trapping at D sites; D_2, free-hole recombination with electrons trapped at D sites.

The free-electron concentration n is obtained from Eq. (5a). Substituting for p from Eq. (5f), the differential equation is in the form of

$$dn/dt = -kn^2 - kbn + X \ , \tag{6}$$

where

$$kb = (C_1 N_C + D_1 N_D) - (C_1 - k)n_C - (D_1 - k)n_D + (H_2 - k)p_H \tag{7}$$

and a similar expression is obtained for p, with kB replacing kb,

$$kB = H_1 P_H - (H_1 - k)p_H + (C_2 - k)n_C + (D_2 - k)n_D \ . \tag{8}$$

The equilibrium concentrations of free carriers become

$$\chi = n(t \to \infty) = X/kb \tag{9a}$$

and

$$\psi = p(t \to \infty) = X/kB \ . \tag{9b}$$

Bleaching of an electron trap can be obtained even when all rate constants, except D_2, are equal,

$$H_1 = H_2 = C_1 = C_2 = D_1 = k \ , \tag{10a}$$

and

$$D_2 \ll k \ . \tag{10b}$$

Equation (10b) implies that the electron trapped at the D site does not recombine, and n_D will saturate at N_D. Under these conditions the free carrier equilibrium values, Eqs. (9), reduce to

$$\chi = X/kP_H \quad \text{and} \quad \psi = X/k(P_H - n_D) \ . \tag{11}$$

Substituting Eq. (11) for n and p into Eq. (5e), integrating, and applying the initial condition $n_D = 0$ at $t = 0$, we get the equation for the occupied fraction of D sites

$$n_D/N_D = 1 - z \ , \tag{12a}$$

where

$$z = \exp(-x) \tag{12b}$$

and the dose x is defined as

$$x = Xt/P_H \ . \tag{12c}$$

The expression shows the expected exponential saturation of the D defects. The equation for the concentration of the C defects becomes

$$n_C/N_C = \frac{1}{1+2\alpha}\left[\alpha + z - (\alpha+1)z\left[\frac{(\alpha+1)z}{\alpha+z}\right]^{1+1/\alpha}\right] , \tag{13}$$

where

$$\alpha = N_C/N_D \tag{14}$$

is the ratio of the C- to D-site densities. Similarly, the H-defect concentration is given by

$$p_H/P_H = \frac{1}{1+2\alpha}\left[\alpha+1-z-\alpha z\left[\frac{(\alpha+1)z}{\alpha+z}\right]^{1+1/\alpha}\right]. \quad (15)$$

The magnitude of the bleaching depends strongly on α; the smaller α, the larger the decay. The measured dose dependence of ΔQ_m^{-1} and EPR Ge(C)-Li data compares reasonably well with n_C/N_C calculated with $\alpha=0.1$. This implies that D sites are much more numerous than C sites, $N_D=0.91P_H$ and $N_C=0.09P_H$. Figure 9 shows the occupied fraction of H, C, and D sites as a function of dose for $\alpha=0.1$. It shows that the C-defect electron center bleaches but both the hole and D-defect electron centers saturate as a function of dose. Experimentally we find that the hole center bleaches. It is possible that when additional rate constants are allowed to differ, the equations would predict bleaching of both the C and H defects. Furthermore, the portion of Al-M which forms Al-h is reduced by the formation of Al-OH, and the rate laws have to include the ion exchange between Al-M and Al-OH. The source of the trapped electrons at the Ge sites is the formation of Al-h, and Ge(C)-Li density is then determined by the aluminum concentration, 0.5 ppm, regardless of the Ge concentration, 30 ppm. The implication, however, that $N_C=0.09P_H$, that is, that the number of active Ge sites is less than $\frac{1}{10}$ of the Al sites, appears unrealistic.

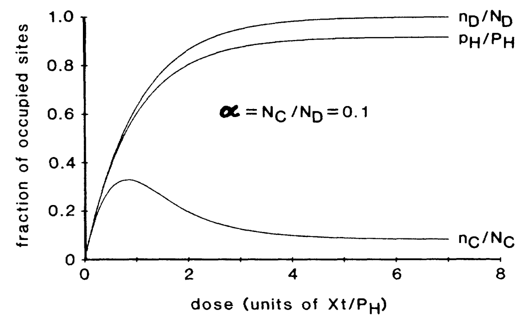

FIG. 9. Fraction of occupied defect sites n_C/N_C, n_D/N_D, and p_H/P_H as a function of dose for $\alpha=N_C/N_D=0.1$.

CONCLUSIONS

We have shown the existence of a new irradiation-induced anelastic loss peak at 246 K, at a resonator frequency of 5 MHz, with activation energy $E=0.22$ eV. The loss peak grows with dose, reaches a maximum at approximately 50 krad, and decays with increasing dose. We suggest that this peak is caused by the Ge(C)-Li center. We have also shown that in high-purity quartz, germanium contamination is very detrimental to oscillator performance. For quartz utilized in high-precision resonator applications Al-impurity concentration is determined by EPR on an irradiated sample. The same evaluation technique will also reveal the presence of Ge-related defects. This investigation points out the importance of combining material characterization and device-performance studies. Without knowledge of complete crystal growth history, or access to characterization records, we would have been unable to explain the unexpected large radiation sensitivity that we have found in devices fabricated from this particular sample of very low-Al-impurity quartz.

ACKNOWLEDGMENTS

We wish to thank our colleagues at Rome Air Development Center (RADC), A. F. Armington, J. J. Larkin, and M. T. Harris for growing the quartz and discussions of their data; J. T. Schott, S. D. Mittleman, J. R. Cappelli, and A. W. Smith for providing the radiation services; and R. J. Andrews, L. D. Diaco, and W. L. Burke for capable technical assistance with resonator and oscillator measurements. We are also indebted to L. E. Halliburton, J. J. Martin, and A. S. Nowick for stimulating and helpful discussions.

[1]B. R. Capone, A. Kahan, R. N. Brown, and J. R. Buckmelter, IEEE Trans. Nucl. Sci. **NS-17**(6), 217 (1970).

[2]J. C. King and H. H. Sander, Radiat. Eff. **26**, 203 (1975).

[3]P. Pellegrini, F. K. Euler, A. Kahan, T. M. Flanagan, and T. F. Wrobel, IEEE Trans. Nucl. Sci. **NS-25**, 1267 (1978).

[4]D. R. Koehler and J. J. Martin, J. Appl. Phys. **57**, 5205 (1985).

[5]J. C. King, J. C. Koehler, and D. R. Koehler, in *Precision Frequency Control,* edited by E. A. Gerber and A. Ballato (Academic, New York, 1985), Chap. 3, pp. 147—159.

[6]D. L. Griscom, in *Proceedings of the 33rd Annual Frequency Control Symposium, 1979,* p. 98. Available from Electronic Industries Association, 2001 Eye St., Washington, D.C. 20006.

[7]J. A. Weil, Phys. Chem. Minerals **10**, 149 (1984).

[8]L. E. Halliburton and J. J. Martin, in *Precision Frequency Control,* edited by E. A. Gerber and A. Ballato (Academic, Orlando, 1985), Chap. 1, pp. 1—45.

[9]J. H. Mackey, J. Chem. Phys. **39**, 74 (1963). The notation inside the square bracket identifies the substitutional impurity, the trapped carrier charge, the presence of interstitial ions (after a virgule), and the net charge on the complex by a superscript. The parenthetical symbol distinguishes centers of similar basic composition and indicates that two distinct lattice defect centers exist. For example, $[\mathrm{Ge}(C)e^-/\mathrm{Li}^+]^0$ describes a neutral defect of a trapped electron localized on a substitutional Ge site and an interstitial Li^+ ion. This is to be distinguished from the $[\mathrm{Ge}(A)e^-/\mathrm{Li}^+]^0$ center.

[10]J. H. Anderson and J. A. Weil, J. Chem. Phys. **31**, 427 (1959).

[11]Y. Haven, A. Kats, and J. S. Van Wieringen, Philips Res. Rep. **21**, 446 (1966).

[12]L. I. Tsinober, M. I. Samoilovich, and L. A. Gordienko, Kristallografiya **10**, 879 (1965) [Sov. Phys.—Crystallogr. **10**, 732 (1966)].

[13]J. C. King, Bell Syst. Tech. J. **38**, 573 (1959).

[14]J. C. King, A. A. Ballman, and R. A. Laudise, J. Phys. Chem. Solids **23**, 1019 (1962).

[15]J. C. King, U.S. Patent No. 3 113 224 (3 December 1963).

[16]J. C. King, U.S. Patent No. 3 932 777 (13 January 1976).

[17]B. R. Capone, A. Kahan, and B. Sawyer, in *Proceedings of the 25th Annual Frequency Control Symposium, 1971,* p. 109. Available as a book or microfiche, document no. AD746211, from NTIS, Sills Building, 5285 Port Royal Road, Springfield, VA 22161.

[18]D. B. Fraser, J. Appl. Phys. **35**, 2913 (1964).

[19]D. B. Fraser, in *Physical Acoustics,* edited by W. P. Mason (Academic, New York, 1968), Vol. 5, Chap. 2, pp. 59–110.

[20]F. Euler, P. Ligor, A. Kahan, and P. Pellegrini, in *Proceedings of the 32nd Annual Frequency Control Symposium, 1978,* p. 24. Available from Electronic Industries Association, 2001 Eye St., Washington, D.C. 20006.

[21]J. J. Martin and S. P. Doherty, in *Proceedings of the 34th Annual Frequency Control Symposium, 1980,* p. 81. Available from Electronic Industries Association, 2001 Eye St., Washington, D.C. 20006.

[22]J. J. Martin, J. Appl. Phys. **56**, 2536 (1984).

[23]A. Kats, Philips Res. Rep. **17**, 133 (1962).

[24]R. N. Brown and A. Kahan, J. Phys. Chem. Solids **36**, 467 (1975).

[25]H. G. Lipson and A. Kahan, J. Appl. Phys. **58**, 963 (1985).

[26]L. E. Halliburton, N. Koumvakalis, M. E. Markes, and J. J. Martin, J. Appl. Phys. **52**, 3565 (1981).

[27]R. H. D. Nuttall and J. A. Weil, Can. J. Phys. **59**, 1696 (1981).

[28]L. E. Halliburton, M. E. Markes, and J. J. Martin, in *Proceedings of the 34th Annual Frequency Control Symposium, 1980,* p. 1. Available from Electronic Industries Association, 2001 Eye St., Washington, D.C. 20006.

[29]S. P. Doherty, S. E. Morris, D. C. Andrews, and D. F. Croxall, in *Proceedings of the 36th Annual Frequency Control Symposium, 1982,* p. 66. Available as a book or microfiche, document no. ADA130811, from NTIS, Sills Building, 5285 Port Royal Road, Springfield, VA 22161.

[30]A. F. Armington and J. F. Balascio, in *Proceedings of the 38th Annual Frequency Control Symposium, 1984,* p. 3. Available as a book or microfiche, document no. 84CH2062-8, from IEEE, 445 Hoes Lane, Piscataway, NJ 08854.

[31]A. F. Armington and J. J. Larkin, J. Cryst. Growth **71**, 799 (1985); **75**, 122 (1986).

[32]J. A. Horrigan (private communication).

[33]The EPR analysis was performed by L. E. Halliburton at Oklahoma State University.

[34]H. G. Lipson, in *Proceedings of the 40th Annual Frequency Control Symposium, 1986,* p. 63. Available as a book or microfiche, document no. 86CH2330-9, from IEEE, 445 Hoes Lane, Piscataway, NJ 08854.

[35]A. Kahan and H. G. Lipson, in *Proceedings of the 39th Annual Frequency Control Symposium, 1985,* p. 255. Available as a book or microfiche, document no. 85CH2186-5, from IEEE, 445 Hoes Lane, Piscataway, NJ 08854.

[36]F. K. Euler, H. G. Lipson, and P. A. Ligor, in *Proceedings of the 34th Annual Frequency Control Symposium, 1980,* p. 72. Available from Electronic Industries Association, 2001 Eye St., Washington, D.C. 20006.

[37]J. J. Martin, H. B. Hwang, and H. Bahadur, in *Proceedings of the 39th Annual Frequency Control Symposium, 1985,* p. 266. Available as a book or microfiche, document no. 85CH2186-5, from IEEE, 445 Hoes Lane, Piscataway, NJ 08854.

[38]J. M. Stevels and J. Volger, Philips Res. Rep. **17**, 283 (1962).

[39]J. M. Stevels, in *Dispersion and Absorption of Sound by Molecular Processes,* Proceedings of the International School of Physics "Enrico Fermi," Course XXVII, Varenna, edited by D. Sette (Academic, New York, 1963), pp. 368–392.

[40]J. A. Weil and J. H. Anderson, J. Chem. Phys. **35**, 1410 (1961).

[41]J. Isoya, J. A. Weil, and R. F. C. Claridge, J. Chem. Phys. **69**, 4876 (1978).

[42]J. H. Anderson, F. J. Feigl, and M. Schlesinger, J. Phys. Chem. Solids **35**, 1425 (1974).

[43]J. Toulouse and A. S. Nowick, J. Phys. Chem. Solids **46**, 1285 (1985).

[44]E. G. S. Paige, Philos. Mag. **2**, 864 (1957).